Comparison of the Physical Characteristics of I-131 and I-123, with Respect to Differentiating the Relative Activity in the Kidneys

Laurence P. Clarke, Farhad Qadir, Wajih Al-Sheikh, George Sfakianakis, and Aldo N. Serafini

University of Miami School of Medicine, Miami, Florida

Iodine-123 (159 keV, $T_{1/2}$ = 13.3 hr) has been proposed for renal investigations, as opposed to I-131 (364 keV, $T_{1/2}$ = 8.06 days), because of its more practical photon energy and lower radiation dose to the patient. The cyclotron production method ^{124}Te $(p,2n)$ ^{123}I for I-123 results in contamination with I-124 ($T_{1/2}$ = 4.5 days). The latter emits high-energy photons whose relative abundance increases with time after end of bombardment (EOB). This paper is an evaluation of the effects of photon penetration, scatter, and attenuation on the phantom calibration measurements required for determining relative renal uptake using I-123. Measurements using I-131 were performed for comparison. Parameters investigated included: (a) the relationship between the integrated count and ROI size, (b) the magnitude of the "cross-talk" in counts between the kidneys, and (c) the attenuation corrections for source (kidney) depth. Phantom results obtained for I-123 suggest that this radionuclide will allow a better measurement of the activity in individual kidneys. Collimator penetration effects were greater for I-131 than for I-123. With I-123 for example, a higher fraction of the counts due to the activity in the kidney phantom were observed within the ROI enclosing its image. However, the attenuation corrections for source depth for I-123 were dependent on both the size of the ROI and time after EOB.

J Nucl Med 24: 683–688, 1983

Iodine-123 (159 keV, $T_{1/2}$ = 13.3 hr) has been proposed for renal investigations, as opposed to I-131 (364 keV, $T_{1/2}$ = 8.02 days), because its principle photon energy should permit better spatial resolution with the gamma camera (*1–3*). In addition, the radiation exposure to the patient is considerably lower for I-123. However, the cyclotron production method ^{124}Te $(p,2n)$ ^{123}I produces an I-124 contaminant, which emits a wide range of high-energy photons (*2–5*). Although the relative amount of I-124 contamination is small at short times after end of bombardment (EOB) (typically 4% at 24 hr), its half-life (4.15 days) is longer than that of I-123. The relative abundance of the high-energy photons therefore increases with time. Because of their energy they will influence: (a) the extent of photon penetration through the detector's collimator, (b) the nature of photon scattering, and (c) the value of the attenuation corrections for the relative depth of the kidneys for I-123 (*2–12*).

In more practical terms, the above factors for I-123 will influence the ability to measure the relative activity in the kidneys. For example, one must consider the following points when flagging a region of interest (ROI) over the kidney to obtain the integrated count. The first is related to the fraction of the total counts detected by the gamma camera, due to the activity in the kidney obtained within: (a) the ROI area enclosing the image of the kidney, and (b) outside the ROI area (*7*). The latter counts will contribute, in part, to a "background count" outside the image boundary of the kidney. Secondly, is the extent of "cross talk" in counts from the activity in the opposite kidney. Third is the "background

Received April 7, 1982; revision Oct. 7, 1982.

For reprints contact: Laurence P. Clarke, PhD, Div. of Nuclear Medicine (D-57), Dept. of Radiology, University of Miami School of Medicine, PO Box 016960, Miami, FL 33101.

counts" detected within the ROI due to the activity in adjacent (or overlapping) organs such as the liver and spleen.

This paper is therefore an evaluation of the effects of photon penetration, scatter, and attenuation on the phantom calibration measurements required for determining relative renal uptake using I-123 and I-131. Phantom measurements were performed in both air and scattering medium to differentiate effects due to scattering and collimator penetration. Specific parameters investigated for both radionuclides included: (a) the relationship between the integrated count and ROI size, (b) magnitude of "cross-talk" in counts between adjacent sources and, (c) attenuation corrections for source depth.

MATERIALS AND METHODS

Radionuclide production. Iodine-123 and I-131 were procured commercially.* The method of production for I-123 and the relative abundance of the photon energies emitted are shown in Table 1. The principal photon energy for I-131 was 365 keV, and for I-123, 159 keV. All measurements were performed with a 20% energy window centered on the main photopeak. The relative magnitude of the I-124 contamination in the production of I-123 is also shown in Table 1. The proportion increased from approximately 4.4% at 28 hr after end of bombardment (EOB) to 18.1% at 63 hr.

Gamma camera/computer system. The camera† had a NaI (Tl) crystal ½ inch thick. It was equipped with a standard Searle high-energy collimator designed for 400 keV. This collimator was used for both I-131 and I-123 (*2*). The camera was interfaced to a computer‡ equipped with a 32K memory and two 2.5-Mbyte discs. The phantom data were acquired as a 64 × 64 word-mode matrix.

The computer was equipped with rectangular region-of-interest (ROI) selection, which was used to enclose the image of each source and obtain the integrated count. The ROI integrated count was normalized to counts per minute and corrected for decay where appropriate. Computer software was generated to select automatically rectangular ROIs of increasing size until the entire sensitive area of the camera was reached. It was therefore possible to determine the relationship between the size of the ROI and the integrated count. Specific regions of interest were identified. First, a rectangular area, of fixed dimensions, chosen to enclose fully the image of the source, for all phantom measurements. This area is referred to as the image area (IA). Second, the rectangular area enclosing the entire sensitive area of the camera crystal. This area is referred to as the total area (TA).

Phantom measurements. Cylindrical sources made from Plexiglas were used to simulate the approximate size of a normal kidney (5 cm diameter, 11 cm long). These sources were supported in a tank (Dimensions: 30 × 30 × 30 cm deep). The tank was mounted on top of the collimator with the camera head inverted. An air gap of 10 mm was maintained between the tank base and collimator face. Source position was measured as the vertical distance from the face of the collimator.

The following measurements were performed for I-123 both in air and in the water tank. First, the source was imaged at a fixed distance of 10 cm from the collimator. The relationship between the size of the integration area (ROI) and the integrated count was investigated. This measurement was then repeated at various times after EOB (23,36,48,63 hr) to determine how time affected the above relationship. Second, the source was imaged at various depths in the tank (5–23 cm from the collimator) to determine the appropriate attenuation corrections for source depth. The corrections were calculated for the two integration areas of interest: the total area (TA) and the image area (IA) as defined earlier.

For all the sources imaged, an accumulated count in excess of 300 k was obtained, to ensure that the random errors in the measurements were small (% s.d.: total integrated count, TA, < ±0.1%, integrated count in image area, IA, < ±0.2%). The systematic errors associated with positioning the source relative to the camera, and with positioning the ROI over the image of the source, were less than ±2%.

The several parameters measured in this study were repeated for the same collimator and for other collimator types, and the observed results were similar, i.e., the

TABLE 1. METHOD OF PRODUCTION OF I-123 AND RELATIVE ABUNDANCE OF PRINCIPAL PHOTON ENERGIES EMITTED (GREATER THAN 1%)

	Reaction:	$^{124}Te^{*}$ $(p, 2n)$	^{123}I		
I-123	Photon energy (keV)	159		529	
	Relative abundance (%)	99		1	
I-124	Contamination (%)	4.4	6.2	10.1	18.1
	Hr after EOB	28	36	48	63

* Highly enriched target.

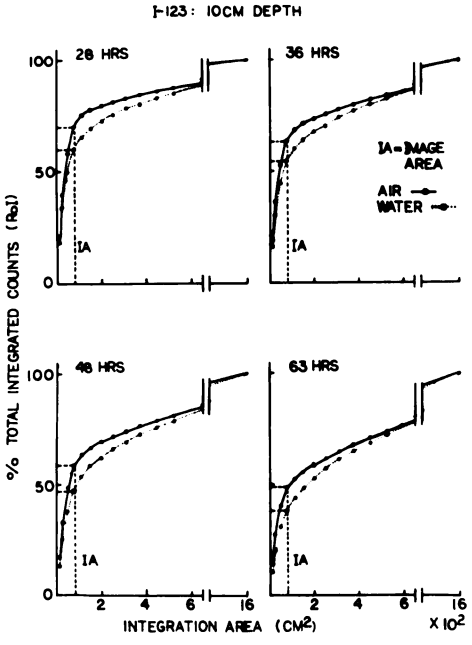

FIG. 1. Influence of size of ROI on observed integrated count for I-123, both in air and in scattering medium. Integrated count for each ROI is expressed as percentage of that obtained for total sensitive area (TA) of camera. Error bars are not shown, since they are less than ±2%.

photon penetration effects for I-123 (I-124 penetration were significant) and yielded results similar to those noted in Figs. 1 and 2. The details of this work will be published in a subsequent article.

Cross-talk index. In the analysis of the calibration measurements, we calculated a cross-talk index (7) to provide an estimate of the level of "cross-talk" in counts between the kidneys for both radionuclides. The index is derived as illustrated in Fig. 4.

$$\text{Percent cross-talk index at separation D} = \frac{C_2}{C_1} \times 100$$

where C_1 is the integrated count within the rectangular area enclosing the image of the source (image area: IA), and C_2 is the integrated count in an adjacent area (AA) of equal size. This index was calculated from the data obtained for the source imaged at a fixed distance of 10 cm from the collimator, and at various times after EOB.

All of the above measurements and calculations were repeated for the I-131 source—though only for one selected time period—for purposes of comparison.

Line spread function (LSF) measurements. The measurements were made to compare the overall spatial resolution of the gamma camera for the two radionuclides. The line source was cylindrical 30 cm long with diameter 2 mm (i.d. of tube). Measurements were made in air at a fixed distance of 10 cm from the collimator face. They were repeated for I-123 for various times after EOB.

RESULTS

Influence of integration area. Figure 1 shows the influence of the size of the integration area (ROI) on the observed integrated count for I-123. The size of the area enclosing the image of the source (IA) is indicated. Results are plotted for various times after EOB. The integrated count was found to increase slowly with increasing ROI size, until the entire sensitive area of the camera was reached. This increase was considered statistically significant, since an accumulated count in excess of 300k was obtained. The percentages of the total integrated count obtained in the image area (IA) are tabulated for air and water in Table 2. The magnitude of this parameter was found to decrease from 60% to 38% at 63 hr after EOB, for the source imaged in the water tank. A large fraction of the counts detected lay outside the image of the source—for example, 62% at 63 hr after EOB. Similar results were observed in air, with only a small increase in counts detected with the image of the source (IA), whose magnitude again decreased with time after EOB.

Figure 2 and Table 2 show the corresponding results obtained for I-131. Again the integrated count increased slowly with increasing ROI size until the total sensitive area (TA) of the camera was reached. However, for I-131, the percentage of the total integrated count within the image of the source (IA) at 48%, was much smaller than for I-123.

Attenuation corrections for source depth. Figure 3 shows the relationship observed for I-123 between the integrated count (log scale) and the position of the source in the water tank. Results were calculated for the area (IA), which was of fixed dimensions, and the total area (TA) of the camera. The integrated count was observed to decrease exponentially with source depth in the tank and therefore permitted "effective" attenuation coefficients to be determined as illustrated in Table 3. The

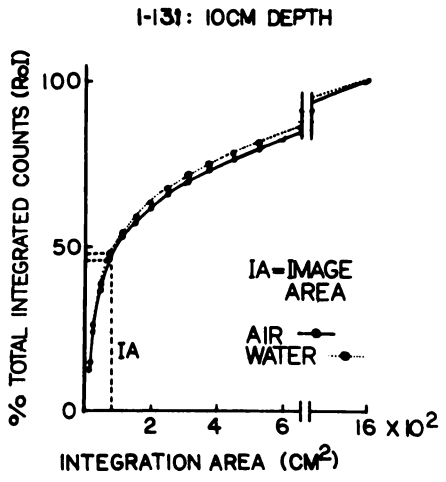

FIG. 2. Influence of size of ROI on observed integrated count for I-131, both in air and in scattering medium. Results are plotted as Fig. 1.

TABLE 2. PERCENTAGE OF TOTAL INTEGRATED COUNT OBTAINED WITHIN AREA ENCLOSING IMAGE OF SOURCE (IA) FOR I-123 AND I-131

Case (A) Fixed depth of 10 cm as in Fig. 1				
	% Integrated count in IA			
Time (hr)	28	36	48	63
I-123: air	70	64	59	49
water	60	55	47	38
I-131: air	47	—	—	—
water	48	—	—	—
Case (B) Fixed Time of 28 hr as in Fig. 2				
Depth (cm)	5	10	15	20
I-123: air	73	70	71	72
water	70	60	52	44
I-131: air	54	47	43	42
water	55	48	42	39

magnitudes of the attenuation coefficients were found to depend both on the ROI size and on the time after EOB.

Cross-talk index. Figure 4 shows schematically how the "cross-talk" index was calculated and the results observed for the two radionuclides. The size of this index was significant at D = 0. For example, for I-123 the cross-talk index at 28 hr was 15%, increasing to 22% at 63 hr. For I-131, a value of 25% at D = 0 was observed. When the value of D = 9 cm was used, typical of the kidney separation in a patient, the values of this index were smaller: 2.5% for I-123 and 5% for I-131.

LSF measurements. Table 4 shows the LSF data. The spatial resolution (FWHM) for I-123 at 28 hr was better than that observed for I-131, but the former degraded with time after bombardment. This was particularly noticeable for the resolution index defined as FWTM (see Table 3), which gives a better indication of the influence of photon penetration through the camera's collimator.

DISCUSSION

The purpose of this paper was to determine emperically the choice of radionuclide for performing quantitative measurements of relative kidney function using the gamma camera. It was not our purpose to investigate photon scattering or collimator penetration effects (septal or corner) in detail. Their theoretical treatment has been reported elsewhere (*9*). The calibration measurements were intended primarily to address the practical problems of measuring relative kidney function.

The results of the calibration data show that the most important physical factors to be considered are collimator penetration and photon attenuation in the water tank. For example, the results in Figs. 1 and 2 were plotted for the sources imaged in air and in the water tank. The large fraction of photons detected outside the image area (IA) can be attributed primarily to photon penetration through the collimator, since the results in the water tank, which also reflects photon-scattering effects, are not very different (see Table 2). The increase in the fraction of photons detected outside the image area for I-123 at greater times after EOB can be attributed to the increase in the relative abundance of high-energy photons due to I-124 contamination. Note that although these photon energies lie outside the energy window enclosing the I-123 photopeak, they may contribute to the photopeak count due to partial energy absorption in the detecting crystal (*4*). The decrease in the effective attenuation coefficients with time after EOB for I-123 can also be attributed to the increased relative abundance of the high-energy photons.

Results obtained for I-123 suggest that this radionuclide will allow better measurement of the activity in each kidney. For example, a higher fraction of the total counts due to the activity in the kidney phantom were observed within the ROI enclosing its image (Fig. 1, Table 2). This is important since, in clinical measurements, one is relating the counts within the ROI (image area: IA) to the activity in each kidney. For I-131, a higher fraction of the total counts was observed outside the same ROI. This would suggest, in turn, that the contribution to the "background count" outside the ROI, due to the activity in the kidney, would be higher for

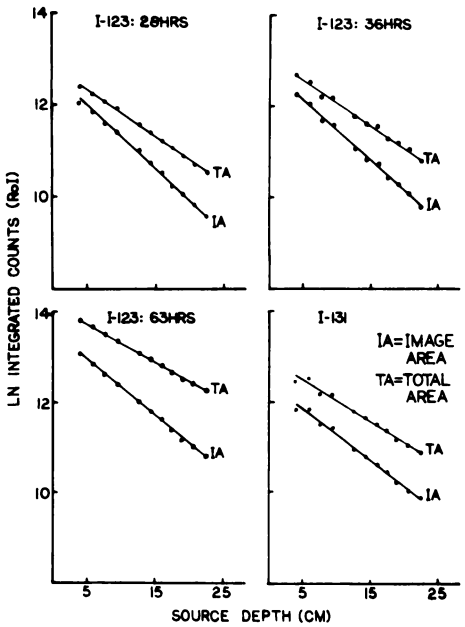

FIG. 3. Influence of size of ROI on attenuation correction required for source depth, for both radionuclides. Results are shown for various times after EOB for I-123. Error bars are not shown because they are less than ±2%.

TABLE 3. CALCULATED ATTENUATION COEFFICIENTS REQUIRED TO CORRECT FOR DEPTH OF SOURCE IN PHANTOM, BASED ON DATA SHOWN IN FIG. 3. FOR I-123 AND I-131. μ_{TA} = ATTENUATION COEFFICIENT FOR TOTAL INTEGRATION AREA (TA); μ_{IA} = ATTENUATION COEFFICIENT FOR IMAGE AREA (IA); s.e. = STANDARD ERROR (11 Experimental Points)

Time (hr)	28	s.e.	36	s.e.	63	s.e.
I-123						
μ_{TA} cm^{-1}	0.105	(0.19)	0.102	(0.19)	0.087	(0.16)
μ_{IA} cm^{-1}	0.139	(0.25)	0.136	(0.25)	0.129	(0.24)
I-131						
μ_{TA} cm^{-1}	0.118	(0.18)	—	—	—	—
μ_{IA} cm^{-1}	0.095	(0.22)	—	—	—	—

I-131 (Fig. 2, Table 2). Furthermore, although sources of larger volume were not scanned, it is reasonable to assume that the "background count" attributed to the presence of active adjacent (or overlapping) organs will be higher for I-131, because of the increased collimator penetration experienced (Fig. 2). The above factors give rise to an uncorrectable source of background activity. Any background correction applied will significantly influence the measurement of relative organ activity (*2,3,7,13–18*).

The results also suggested that the level of "cross talk" in counts between the kidneys should be less for I-123, particularly at early times after EOB (Fig. 4). However, the magnitude of this factor was not very significant for a typical kidney separation of 9 cm. The one disadvantage observed for I-123 was the fact that the attenuation corrections for source depth were dependent on both the size of the ROI used and the time after EOB. Careful calibration measurements are therefore required for renal work with I-123, especially if variable regions of interest (ROI) are used or if it is planned to use the I-123 tracer more than 24 hr after EOB. These problems are even more significant if one proposes to use I-123 to make quantitative measurements of small organs such as the adrenals with the gamma camera (*7,18*).

Several parameters were not considered in this work. For example, the selection of the optimum integration area (ROI) to permit an approximate correction for active tissue background surrounding the kidneys was not considered. In the calibration measurements, the "background count" contribution due to activity above and below the kidneys (due to circulating blood), was also not considered. Volume sources of cylindrical shape were used to simulate the size of the kidney. If one wished to investigate specifically the optimum choice of ROI area for quantitative renal measurements in more detail, such as the use of isocount contours (*13*), a more realistic phantom model would be required. Furthermore, for the attenuation measurements in the water tank (Fig. 3), we used an integration area (image area: IA) of fixed dimensions, fully enclosing the image of the source. The attenuation corrections would have a greater variation with depth if ROIs closer to the source's

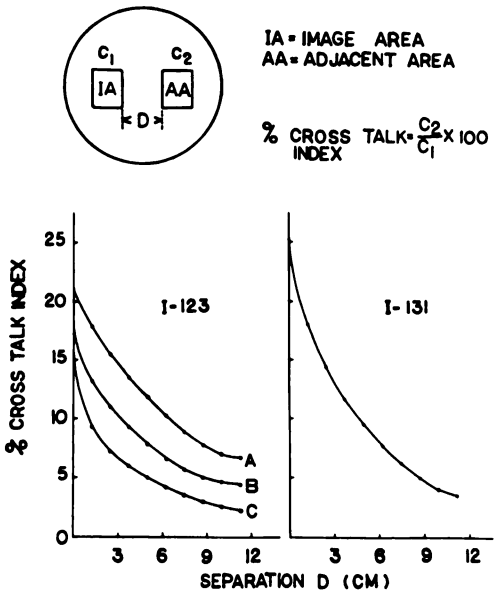

FIG. 4. Comparison of "cross-talk" indices, as defined in text. Results are shown for various times after EOB for I-123: (A) 63 hr, (B) 48 hr, (C) 28 hr.

TABLE 4. COMPARISON OF RESULTS OBTAINED FOR LSF MEASUREMENTS. DATA WERE OBTAINED FOR 10-CM DEPTH IN AIR. RESULTS FOR I-123 ARE SHOWN FOR VARIOUS TIMES AFTER EOB

I-123	EOB	FWHM* (cm)	FWTM† (cm)
	28 hr	2.2	3.25
	48 hr	2.4	3.75
I-131	—	3.1	4.5

* FWHM = Full width half maximum.
† FWTM = Full width tenth maximum.

cross-sectional area were used of if the isocount contours had reflected more closely the image size (*7,13*). Fixed rectangular integration areas were used in this work to simplify the intepretation of the results. The conclusions reached here apply to the production methods for our particular I-123. If it were produced by an on-site medical cyclotron, the above data could be analyzed at earlier times after EOB, with a corresponding reduction in the amount of I-124 contamination.

To summarize, the above measurements were considered important because of the proposed use of I-123 for radiorenograms, and the increasing interest in performing differential glomerular filtration rate or differential measurements of effective renal plasma flow (*19*).

FOOTNOTES

* E. R. Squibb & Sons, Inc., and Medical Physics, Inc., respectively.

† Searle large field of view (LFOV).

‡ Medical Data Systems PAD.

REFERENCES

1. HOLYROYD AM, CHRISHOLM GD, GLASS HI: The quantitative analysis of renograms using the gamma camera. *Phys Med Biol* 15:483-492, 1970
2. ZIELINSKI FW, HOLLY FE, ROBINSON GD, et al: Total and individual kidney function assessment with iodine-123 ortho-iodohippurate. *Radiology* 125:753-759, 1977
3. SHORT MD, GLASS HI, CHRISHOLM GD, et al: Gamma camera renography using I-123 hippuran. *Br J Radiol* 46: 289-294, 1973
4. KENNY PJ: Physical factors involved in imaging iodine-123 distributions. In *Thyroid and Endocrine System Investigations with Radionuclides and Radioassays.* F. S. Ashkar, Ed. Masson Publishing USA, Inc., New York, 1979, p 14
5. BEAVER JE: I-123 production and availability. In *Thyroid and Endocrine System Investigations with Radionuclides and Radioassays.* F. S. Ashkar, Ed. Masson Publishing USA, Inc., New York, 1979, p 24
6. SANKEY RR, READ ME: Physics of I-123 imaging and the role of the computer in the thyroid workshop. In *Thyroid and Endocrine System Investigations with Radionuclides and Radioassays.* F. S. Ashkar, Ed. Masson Publishing USA, Inc., New York, 1979, p 36
7. CLARKE LP, MALONE JF, CASEY M: Quantitative measurement of activity in small sources containing medium energy radionuclides: Comparison of the gamma camera and the rectilinear scanner. *Br J Radiol* 55:125-133, 1982
8. CLARKE LP, SERAFINI AN: Relative and absolute uptake measurements with the gamma camera: An assessment of errors. *J Nucl Med* 21: P 82 (abst)
9. BECK RN: Collimation of gamma rays. In *Fundamental Problems in Scanning.* Cottschalk A, Beck RN, Eds. Charles C. Thomas, Springfield, 1968, 71-92
10. NIMMON CC, MCALLISTER JM, CATTEL WR: Kidney position and the measurement of relative uptake of I-131 hippuran in renography. *Br J Radiol* 48:286-290, 1975
11. OSTROWSKI ST, TOTHILL P: Kidney depth measurements using a double isotope technique. *Br J Radiol* 48:291-294, 1975
12. KORAL KF, JOHNSTON AT: Estimation of organ depth by gamma ray spectral comparison. *Phys Med Biol* 22:988-993, 1977
13. CLARKE LP, MAUGHAM EZ, LAUGHLIN JS: Calibration methods for measuring splenic sequestration by external scanning. *Med Phys* 3:324-327, 1976
14. FARMELANT MH, BURROWS BA: The renogram: Physiological basis and current clinical use. *Semin Nucl Med* 4: 61-73, 1974
15. RAYNAUD C: A technique for the quantitative measurement of the function of each kidney. *Semin Nucl Med* 4:51-60, 1974
16. SFAKIANAKIS GN, SFAKIANAKIS E, MINER GW: Radioisotope kidney studies in pediatric age (comparison between ^{99m}Tc-DTPA and ^{131}I-hippurate, In *Proc Sym on Sharing of Computer Programs and Technology in Nuclear Medicine, Computer Assisted Date Processing*, Atlanta, Georgia, January 1977, pp 125-130
17. BRITTON KE, BROWN NJ: The clinical use of C.A.B.B.S. renography. *Br J Radiol* 41:570-579, 1968
18. MORITA R, LIEBERMAN LM, BEIERWALTES WH, et al: Percent uptake of I-131 radioactivity in the adrenal from radioiodinated cholesterol. *J Clin Endocrinol Metab* 34:36-43, 1972